

See discussions, stats, and author profiles for this publication at: <https://www.researchgate.net/publication/239288991>

# Gadolinium–environment in borate–tellurate glass ceramics studied by FTIR and EPR spectroscopy

ARTICLE *in* JOURNAL OF NON-CRYSTALLINE SOLIDS · MARCH 2010

Impact Factor: 1.77 · DOI: 10.1016/j.jnoncrysol.2009.12.011

CITATIONS

13

READS

76

## 4 AUTHORS:



**Simona Rada**

Universitatea Tehnica Cluj-Napoca

82 PUBLICATIONS 902 CITATIONS

SEE PROFILE



**V. Dan**

11 PUBLICATIONS 71 CITATIONS

SEE PROFILE



**Marius Rada**

National Institute for Research and Develo...

44 PUBLICATIONS 332 CITATIONS

SEE PROFILE



**Eugen Culea**

Universitatea Tehnica Cluj-Napoca

180 PUBLICATIONS 1,671 CITATIONS

SEE PROFILE



# Gadolinium-environment in borate–tellurate glass ceramics studied by FTIR and EPR spectroscopy

S. Rada \*, V. Dan, M. Rada, E. Culea

Technical University of Cluj-Napoca, 400641 Cluj-Napoca, Romania

## ARTICLE INFO

### Article history:

Received 30 January 2009

Received in revised form 2 December 2009

Available online 11 January 2010

### Keyword:

Glass ceramics

## ABSTRACT

Modifications of the gadolinium-environment in borate–tellurate glass ceramics system, where  $0 \leq x \leq 30$  mol%, under heat treatment have been investigated by FTIR and Electron Paramagnetic Resonance (EPR) spectroscopy. Glass ceramics with a molar composition of  $x\text{Gd}_2\text{O}_3 \cdot (100 - x)[6\text{TeO}_2 \cdot 4\text{B}_2\text{O}_3]$  where  $0 \leq x \leq 30$  mol%, was prepared by one-step crystallization heat treatment of the parent glass at temperatures of 400 and 475 °C, respectively. After the heat treatment applied at 400 °C, some structural changes were observed and the  $\text{B}_2\text{O}_3$  crystalline phase appeared in the structure of the samples. The crystallization of the  $\text{B}_2\text{O}_3$  crystalline phase increases with increasing of the gadolinium concentration because the excess of the oxygen yields the formation of free  $\text{BO}_3^{3-}$  orthoborate units capable for charge compensation of the gadolinium ions. By increasing of the treatment temperature up to 475 °C, the increase of the capacity of migration inside the glass ceramics network yields the apparition of  $\text{B}_2\text{O}_3$  and  $\text{TeO}_2$  crystalline phases. When a higher  $\text{Gd}_2\text{O}_3$  content is introduced, more  $[\text{BO}_3]$  structural units are coupled with gadolinium ions, the Te–O–Te linkages are deformed showing that the  $\text{Gd}_2\text{O}_3$  behaves as a glass-former by means of the intercalation of  $[\text{GdO}_4]$  entities in the  $[\text{TeO}_4]$  chain network. The changes produced by devitrification suggest the competition between cations of tellurium and boron with non-bridging oxygens to compensate the positive charge of the gadolinium ions. Thus, gadolinium ions play a dual role of network former (475 °C) and network modifier (400 °C) in the studied samples

© 2009 Elsevier B.V. All rights reserved.

## 1. Introduction

The recent interest in the preparation of the family of materials known as glass–ceramics arises from the fact that glasses are less prone than ceramics to processing flaws arising from packing defects. The large agglomerates can produce flaws in the sintering ceramics [1,2], but glasses usually sinter to full density even when the immature microstructure is non-uniform. Therefore, in the optimum process for preparation of glass–ceramics, the glass should form to full density before the onset of crystallization.

The glass crystallization method by thermal treatments is attractive because it can be conducted at lower temperatures and allows greater control over phase separation and crystallization. It seems the necessary to study the relationship between thermal treatments and crystalline phase formation.

Glasses based on heavy metal oxide such as  $\text{TeO}_2$  have wide applications in the field of glass ceramics, layers for optical and

electronic devices, thermal and mechanical sensors, reflecting windows [3,4].

$\text{B}_2\text{O}_3$  is one of the most common glass-former [5]. The structure of vitreous  $\text{B}_2\text{O}_3$  consists of a random network of boroxol rings and  $[\text{BO}_3]$  triangles connected by B–O–B linkages [6]. It was reported that addition of a network modifier in borate glasses could produce the conversion of the triangular  $[\text{BO}_3]$  structural units to  $[\text{BO}_4]$  tetrahedral with a coordination number four [7].

The glassy-crystalline materials (or nanomaterials) obtained via direct crystallization from the glassy state are one of the most interesting ceramics materials [8,9]. Glassy-crystalline materials combine advantages of crystalline materials (mechanical strength) and those of amorphous ones (easy processing, controllable properties). Composition, but also structure and texture of the glass have decisive influence on the type and the properties of glassy-crystalline materials.

Design of the controlled crystallization process of gadolinium–borate–tellurate glasses in order to obtain glassy-crystalline materials has been the main goal of the work. The purpose of this paper was to approach the structure of gadolinium–borate–tellurate glass ceramics and to obtain data on the local environment change of  $\text{Gd}^{3+}$  ions. Structural changes of the glass ceramics have been studied using the X-ray diffraction, FTIR and EPR spectroscopy.

\* Corresponding author.

E-mail addresses: [Simona.Rada@phys.utcluj.ro](mailto:Simona.Rada@phys.utcluj.ro), [radasimona@yahoo.com](mailto:radasimona@yahoo.com) (S. Rada).

## 2. Experimental

Glasses with composition  $x\text{Gd}_2\text{O}_3 \cdot (100 - x)[6\text{TeO}_2 \cdot 4\text{B}_2\text{O}_3]$  ( $0 \leq x \leq 30$  mol%) were prepared by conventional melt-quenching method, melting mixtures of  $\text{TeO}_2$ ,  $\text{H}_3\text{BO}_3$  and  $\text{Gd}_2\text{O}_3$  reagents of purity grade in a corundum crucibles at  $800^\circ\text{C}$  for 60 min. Then, the glasses samples were subject to heat treatment applied at  $400^\circ\text{C}$  for 38 h and at  $475^\circ\text{C}$  for 24 h, respectively.

The samples were analyzed by means of X-ray diffraction using a XRD-6000 Shimadzu diffractometer, with a monochromator of graphite for the  $\text{Cu K}\alpha$  radiation ( $\lambda = 1.54 \text{ \AA}$ ) at room temperature.

The structure of the glasses was investigated by infrared spectroscopy using the KBr pellet technique. The IR spectra were recorded in the range  $400\text{--}1600 \text{ cm}^{-1}$  using a JASCO FTIR 6200 spectrophotometer. The spectra were carried out with a standard resolution of  $2 \text{ cm}^{-1}$ .

EPR measurements were performed at room temperature using ADANI Portable EPR PS 8400-type spectrometer, in X frequency band (9.1 GHz) and a field modulation of 100 kHz. The microwave power used was 5 mW. All EPR spectra have been normalized to the samples mass. Error estimation has been done for all data obtained taking into account contribution of the random and systematic errors. Systematic error include uncertainty in the mass measuring (uncertainty of 0.1 mg). In order to minimize the random error measurements of the spectra were repeated 10 times.

## 3. Results

The glass crystallization method is convenient to produce vitroceraamics with pre-determined properties, since their structural properties can be adjusted by the manipulation of the heat treatment conditions. The X-ray diffraction patterns reveal  $\text{B}_2\text{O}_3$  and  $\text{TeO}_2$  crystalline phases in the structure of the treated samples at 400 and  $475^\circ\text{C}$ , respectively (Figs. 1 and 4).

The FTIR spectra of the studied treated  $x\text{Gd}_2\text{O}_3 \cdot (100 - x)[6\text{TeO}_2 \cdot 4\text{B}_2\text{O}_3]$  ( $0 \leq x \leq 30$  mol%) glass ceramics are shown in Figs. 2, 5 and 7. FTIR spectroscopy was used to obtained essential information concerning the arrangement of the structural units of these glasses.

The bands located around  $460 \text{ cm}^{-1}$ , in the range of  $610\text{--}680 \text{ cm}^{-1}$  and  $720\text{--}780 \text{ cm}^{-1}$  are assigned the bending mode of  $\text{Te-O-Te}$  or  $\text{O-Te-O}$  linkages, the stretching mode  $[\text{TeO}_4]$  trigonal

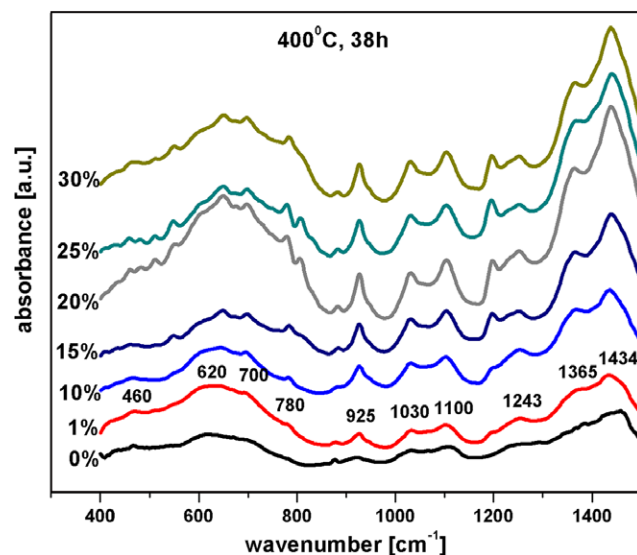


Fig. 2. FTIR spectra of  $x\text{Gd}_2\text{O}_3 \cdot (100 - x)[6\text{TeO}_2 \cdot 4\text{B}_2\text{O}_3]$  glass ceramics treated at  $400^\circ\text{C}$  with  $0 \leq x \leq 35$  mol%  $\text{Gd}_2\text{O}_3$ .

pyramidal with bridging oxygen and the stretching mode of  $[\text{TeO}_3]$  trigonal pyramidal with non-bridging oxygen, respectively [10–13].

It is known that in the vitreous  $\text{B}_2\text{O}_3$  about 80% of the boron atoms are present in the boroxol rings,  $\text{B}_3\text{O}_6$ , that are interconnected by independent  $[\text{BO}_3]$  groups [14]. Thus, vibrational modes of the vitreous borate network are mainly active in three infrared spectral regions. The IR features located in the first region that ranges between  $1200$  and  $1600 \text{ cm}^{-1}$  are due to the asymmetric stretching relaxation of  $\text{B-O}$  bonds of from the  $[\text{BO}_3]$  trigonal units. The second region ranges between  $800$  and  $1200 \text{ cm}^{-1}$  and its spectral features are due to the  $\text{B-O}$  bond stretching of  $[\text{BO}_4]$  tetrahedral units. In the third region ranging from  $400$  to  $800 \text{ cm}^{-1}$  there is an important band located around  $720 \text{ cm}^{-1}$  assigned to the bending vibrations of various borate segments [14–16].

The EPR spectra of  $x\text{Gd}_2\text{O}_3 \cdot (100 - x)[6\text{TeO}_2 \cdot 4\text{B}_2\text{O}_3]$  glass ceramics samples treated at 400 and  $475^\circ\text{C}$  were illustrated in Figs. 3, 6 and 8.

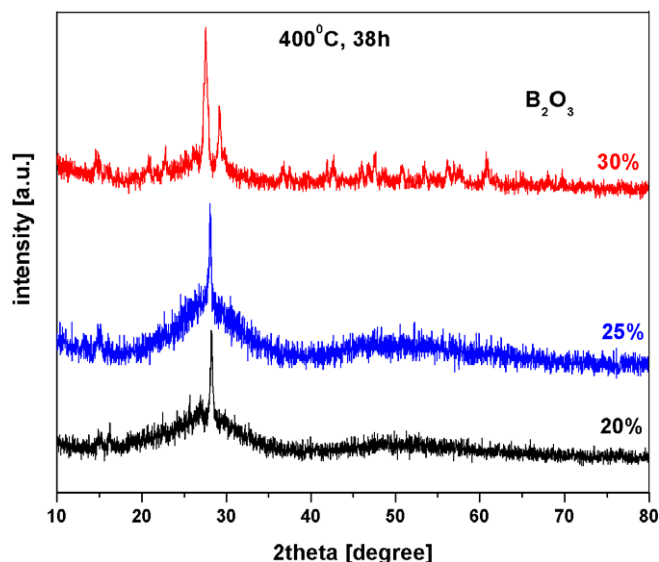


Fig. 1. X-ray diffraction patterns for  $x\text{Gd}_2\text{O}_3 \cdot (100 - x)[6\text{TeO}_2 \cdot 4\text{B}_2\text{O}_3]$  glass ceramics treated at  $400^\circ\text{C}$  with  $x = 20, 25$  and  $30$  mol%.

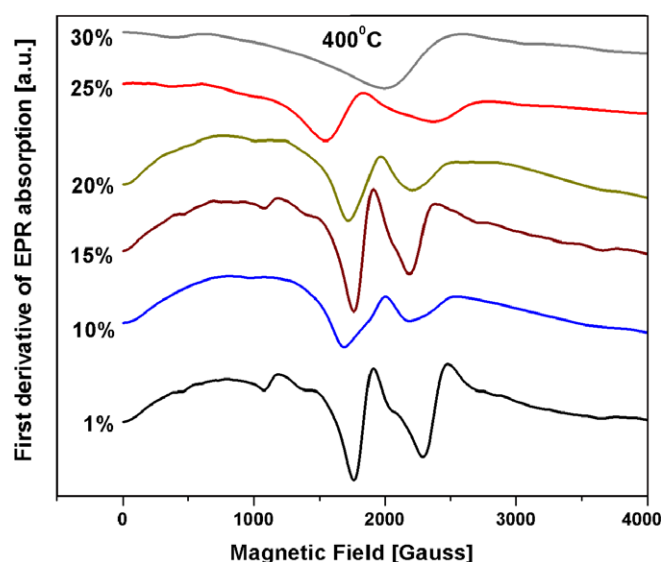


Fig. 3. EPR spectra of  $x\text{Gd}_2\text{O}_3 \cdot (100 - x)[6\text{TeO}_2 \cdot 4\text{B}_2\text{O}_3]$  glass ceramics treated at  $400^\circ\text{C}$ .

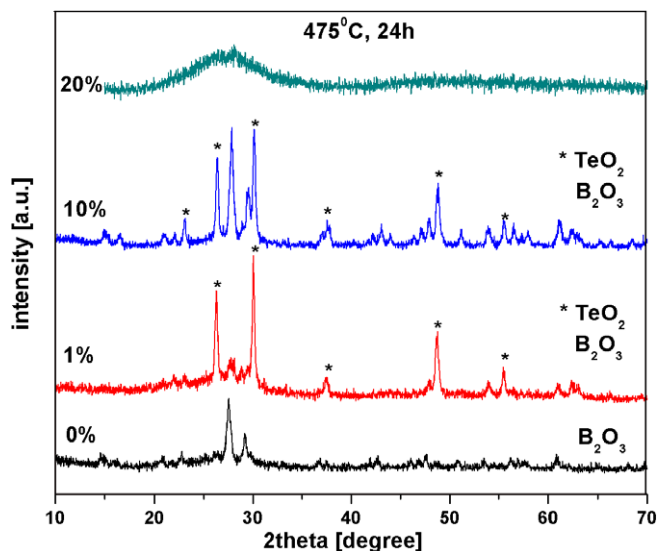


Fig. 4. X-ray diffraction patterns for  $x\text{Gd}_2\text{O}_3 \cdot (100 - x)[6\text{TeO}_2 \cdot 4\text{B}_2\text{O}_3]$  glass ceramics treated at 475 °C with  $x = 20, 25$  and 30 mol%.

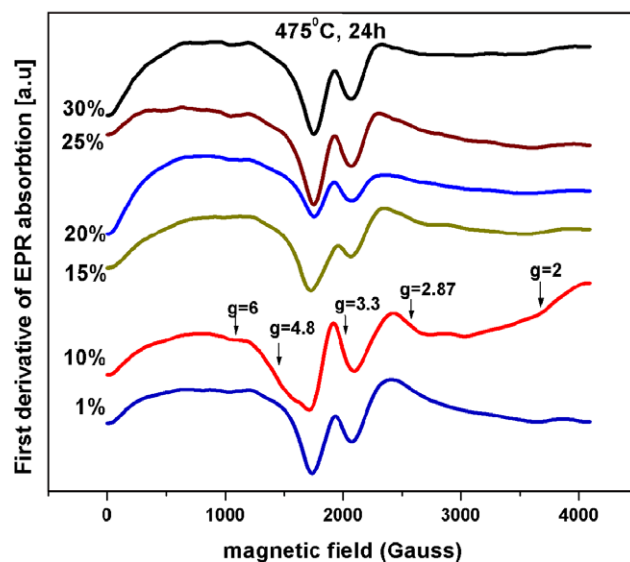


Fig. 6. EPR spectra of  $x\text{Gd}_2\text{O}_3 \cdot (100 - x)[6\text{TeO}_2 \cdot 4\text{B}_2\text{O}_3]$  glass ceramics treated at 475 °C.

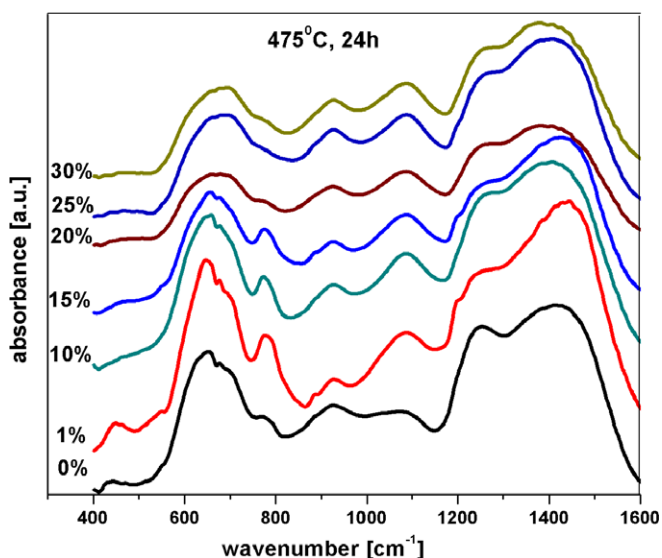


Fig. 5. FTIR spectra of  $x\text{Gd}_2\text{O}_3 \cdot (100 - x)[6\text{TeO}_2 \cdot 4\text{B}_2\text{O}_3]$  glass ceramics treated at 475 °C with  $0 \leq x \leq 35$  mol%  $\text{Gd}_2\text{O}_3$ .

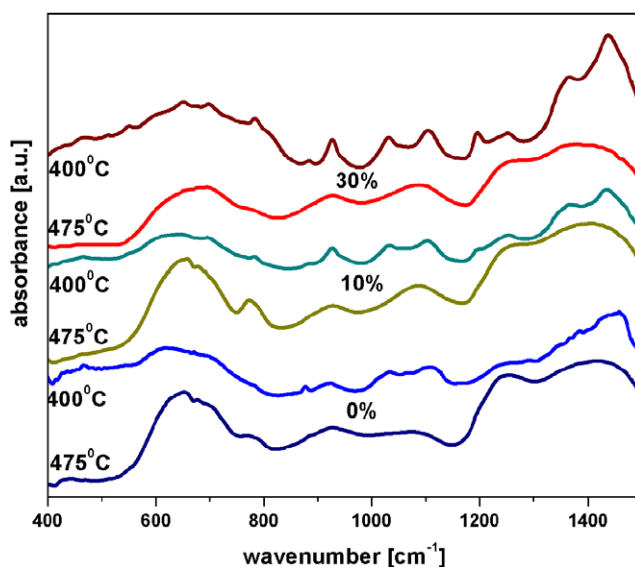


Fig. 7. FTIR spectra of the  $x\text{Gd}_2\text{O}_3 \cdot (100 - x)[6\text{TeO}_2 \cdot 4\text{B}_2\text{O}_3]$  samples treated at 400 and 475 °C.

FTIR and EPR spectroscopy have been used in order to analyze the local structural peculiarities of our samples, to identify the contributions of each component on the structure and to point out the role of the gadolinium ions as a modifier and former on the glass ceramics network.

#### 4. Discussion

##### 4.1. Glass ceramics system treated at 400 °C

The FTIR spectra for the  $x\text{Gd}_2\text{O}_3 \cdot (100 - x)[6\text{TeO}_2 \cdot 4\text{B}_2\text{O}_3]$  ( $0 \leq x \leq 30$  mol%) glass ceramics system treated at 400 °C are presented in Fig. 2. Obtained bands and their assignments can be summarized as follows:

- (i) The large band centered at  $\sim 620 \text{ cm}^{-1}$  is assigned to the stretching mode of  $[\text{TeO}_4]$  trigonal bipyramidal with bridg-

ing oxygens [10,11]. The shoulder located at  $\sim 780 \text{ cm}^{-1}$  indicates the presence of the  $[\text{TeO}_3]$  structural units [12,13].

- (ii) The band located at about  $700 \text{ cm}^{-1}$  results from oxygens bridges forming between one tetrahedral and one trigonal boron atom and between two trigonal boron atoms [14].
- (iii) The broader bands located in  $800\text{--}1200 \text{ cm}^{-1}$  the region are due to the stretching vibrations of the B–O bonds of  $[\text{BO}_4]$  structural units. The feature of band centered at about  $\sim 1030 \text{ cm}^{-1}$  is due to the B–O vibrations of pentaborate, tetraborate, triborate and diborate structural units. The IR band located at about  $1243 \text{ cm}^{-1}$  was attributed to the B–O stretching vibrations of the  $[\text{BO}_3]$  structural units from the boroxol rings [15].
- (iv) The features of the band presented in the  $1300\text{--}1500 \text{ cm}^{-1}$  region can be attributed to the B–O stretching vibrations of  $[\text{BO}_3]$  structural units, which are associated with the vibrational mode inside the various borate rings and the non-

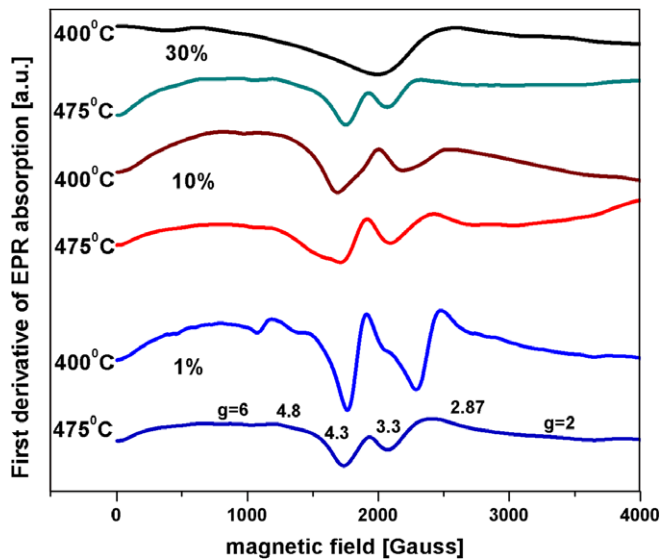


Fig. 8. EPR spectra of the  $x\text{Gd}_2\text{O}_3 \cdot (100 - x)[6\text{TeO}_2 \cdot 4\text{B}_2\text{O}_3]$  samples treated at 400 and 475 °C.

bridging B–O<sup>−</sup> bonds, respectively. This band responsible for non-bridging oxygen atoms increase in the borate units by increasing of the gadolinium ions from host network indicating that more non-bridging oxygen ions exist in borate glass. These stronger vibration bands reflect that more [BO<sub>3</sub>] structural units coupling with gadolinium ions still exist in the glass host. The gadolinium ions have a strong affinity towards the groups containing non-bridging oxygens, which is negative-charged, because they are readily available for charge compensation [16]. Tanabe [17] has pointed out that B–O bonds are formed by an introduction of gadolinium ions itself dominantly coordinate gadolinium ions instead of a large number of boroxol rings.

- (v) The vibration band centered at about  $\sim 925 \text{ cm}^{-1}$  can be assigned to Te–O<sup>−</sup> non-bridging bonds of the [TeO<sub>3</sub>] structural units. However, there are still a lot of gadolinium ions existing in the tellurate units. They can be attributed to the influence of the lone-pair electrons of tellurate units [12]. Then, by increasing of Gd<sub>2</sub>O<sub>3</sub> content, the ratio of the vibrational intensity of [TeO<sub>3</sub>] and [TeO<sub>4</sub>] structural units was changed [18,19].

The increase of the Gd<sub>2</sub>O<sub>3</sub> content does strongly modify the characteristic bands and these could be explained in two proceedings:

- (i) For  $0 \leq x \leq 20 \text{ mol\% Gd}_2\text{O}_3$ , the number of [TeO<sub>4</sub>] structural units increases.
- (ii) For  $x > 20 \text{ mol\% Gd}_2\text{O}_3$ , a [TeO<sub>4</sub>] → [TeO<sub>3</sub>] conversion process takes place.

In brief, by increasing of the Gd<sub>2</sub>O<sub>3</sub> content, [TeO<sub>4</sub>] structural units are transformed into [TeO<sub>3</sub>] structural units and a large number of non-bridging oxygen ions from modifying oxide exist in the host glass. So that, the content of [BO<sub>3</sub>] structural units with non-bridging oxygens increases yielding the appearance of the B<sub>2</sub>O<sub>3</sub> crystalline phase (Fig. 1).

In order to understand the FTIR data concerning to the existence a large number of non-bridging oxygen ions from modifying oxide, we investigated the local environment of the gadolinium ions using EPR spectroscopy.

The EPR spectra of undoped samples show no signals confirming that the starting materials used for base glass ceramics are free from any paramagnetic impurities. Fig. 3 shows the EPR spectra of  $x\text{Gd}_2\text{O}_3 \cdot (100 - x)[6\text{TeO}_2 \cdot 4\text{B}_2\text{O}_3]$  glass ceramics sample treated at 400 °C as function of gadolinium ions concentration. The Gd<sup>3+</sup> ions doped borate–tellurate glass ceramics exhibits six resonance signals at  $g \approx 2.0, 2.8, 3.3, 4.3, 4.8$  and 6.

Most of the authors [20–22] consider that when the gadolinium ions present in low concentrations in host glasses, usually exhibit three prominent signals with effective  $g$ -values of  $g \approx 6, 2.8$  and 2.0 superimposed on a broad resonance line shape that encompasses the prominent  $g \approx 2.0$  resonance signals. The mentioned absorption features are generated by Gd<sup>3+</sup> ions disposed in cubic, octahedral or tetrahedral sites with moderate distortions. In these sites the gadolinium ions experience a relatively weak crystalline field and they are characterized by a coordination number higher than six [23–25].

The asymmetric absorption line with  $g \approx 4.8$  indicates a relatively strong crystal field with an orthorhombic symmetry and is associated with gadolinium ions with a coordination number lower than six [22].

In addition to the signals at  $g \approx 3.3$  and 4.3 are also observed [20]. This type of spectrum has been aptly labeled as the U-spectrum [26] in view of its omnipresence in vitreous materials [20–28] as well as in disordered polycrystalline materials. In the present work, the increase of Gd<sub>2</sub>O<sub>3</sub> content does strongly modify the characteristic bands of the EPR spectra and can be characterized as follows:

- (i) For sample with  $x = 1 \text{ mol\% Gd}_2\text{O}_3$ , the EPR spectra shows all absorption features of the U-spectrum. The three EPR signals at  $g \approx 2, 2.87$  and 6 are due to Gd<sup>3+</sup> ions located at sites with weak, intermediate and strong cubic symmetry fields. In principle these sites may be of network forming [22]. The presence of line at  $g \approx 4.8$  characterized for Gd<sup>3+</sup> ions in sites of strong crystal fields having a low coordination number. This type of Gd<sup>3+</sup> ions can be presented as network former in the glass [29].
- (ii) For  $x > 1 \text{ mol\% Gd}_2\text{O}_3$ , the intensity of EPR lines ( $g \approx 6$ ) corresponding to Gd<sup>3+</sup> in a network modifier position decreases whereas the ones at  $g \approx 4.8$  correlated to Gd<sup>3+</sup> in a network former position increases.

These results suggested that there are two different sites for Gd<sup>3+</sup> ions corresponding to a network former and modifier positions of Gd<sup>3+</sup> in the glass. The gadolinium ions are mainly inserted in the trivalent state and they can be considered as intermediate cations, both network formers and modifiers depending on the glass composition and the oxide gadolinium content. One can see that higher Gd<sub>2</sub>O<sub>3</sub> content affects the Gd<sup>3+</sup> ions in the network former sites.

Therefore Gd<sup>3+</sup> ions will coordinate more with non-bridging oxygens leading the decreased of the number of individual Gd<sup>3+</sup> ions. According to these results, it can be concluded that most of the gadolinium incorporated into the glass is not located inside clusters and the Gd<sup>3+</sup> content is distributed into two sites attributed to network modifier and network former.

#### 4.2. Glass ceramics system treated at 475 °C

The devitrification of the samples at the 400 °C shows the presence of the B<sub>2</sub>O<sub>3</sub> crystalline phase (Fig. 1). The increase of treated temperature up to 475 °C causes significant changes and the appearance of the B<sub>2</sub>O<sub>3</sub> and TeO<sub>2</sub> crystalline phases (Fig. 4). In Fig. 1, the crystallization increases with increasing of the gadolinium concentration. In Fig. 4, the behavior seems to be the opposite.



The changes produced by devitrification suggest the competition between cations of tellurium and boron with non-bridging oxygens to compensate the positive charge of the gadolinium ions.

The role of the boron and tellurium oxides in the geometrical arrangement of the building units of the glass ceramics network can be considered as follows (Fig. 5):

- (i) For low concentrations,  $0 \leq x \leq 20$  mol%, the intensity of the band centered at  $\sim 780 \text{ cm}^{-1}$  increases by increasing of the gadolinium ions concentration. This observation is consistent with the destruction of the  $[\text{TeO}_4]$  structural units. The content of three-coordinated tellurium attains its maximum values of 1 mol%  $\text{Gd}_2\text{O}_3$  yielding the apparition of the  $\text{TeO}_2$  crystalline phase. It seems that the content of  $[\text{BO}_4]$  structural units become higher, because results the transformation of some  $[\text{BO}_3]$  units to  $[\text{BO}_4]$  structural units.
- (ii) The band centered at around  $450 \text{ cm}^{-1}$  is most often assigned to bending vibrations of  $\text{Te-O-Te}$  linkages. The intensity of this band varies with the increasing of the amounts of gadolinium oxide. For sample with  $x > 1$  mol% can be observed a decreasing trend of the strength bands suggesting the destruction of the  $\text{Te-O-Te}$  linkages. The effects suggest that the gadolinium ions deform the  $\text{Te-O-Te}$  linkages and change the distribution of ordered microregions of the glass ceramics. These observations can be consistent with the idea that  $\text{Gd}_2\text{O}_3$  behaves as a glass-former for  $x > 1$  mol%, at these concentrations is an intercalation of  $[\text{GdO}_4]$  entities in the  $[\text{TeO}_4]$  chain network. For  $x \geq 20$  mol%, the numbers of  $[\text{GdO}_4]$ ,  $[\text{BO}_4]$  and  $[\text{TeO}_4]$  structural units increase yielding the apparition of vitreous phase (Fig. 4).

In brief, as the  $\text{Gd}_2\text{O}_3$  content increases, the geometrical arrangement of the building units of the glass ceramics network can be summarized as follows:

- (i) The addition of 1 mol%  $\text{Gd}_2\text{O}_3$  in the glass ceramic matrix lead the increase of the number of  $[\text{TeO}_3]$ ,  $[\text{BO}_4]$  structural units and the formation of the  $\text{TeO}_2$  crystalline phase.
- (ii) For  $1 < x \leq 20$  mol%  $\text{Gd}_2\text{O}_3$ , the intensity of the bands corresponding to the  $[\text{TeO}_3]$  structural units decreases while these corresponding to the  $[\text{BO}_3]$  structural units increase. This mechanism can be due to the conversion of glass ceramic network from  $[\text{TeO}_3]$  units into  $[\text{TeO}_4]$  structural units and the  $[\text{BO}_4]$  units into  $[\text{BO}_3]$  structural units, respectively.
- (iii) The gradual increase of gadolinium oxide in the glass ceramics up to 30 mol% results to the transformation some  $[\text{BO}_3]$  trigonal units to  $[\text{BO}_4]$  tetrahedral structural units.

In brief, it seems that the content of  $[\text{BO}_4]$  structural units cannot become higher, because the modified  $[\text{BO}_3]$  units containing one or more B–O–Gd bonds are unable to accept a fourth oxygen atom. The gadolinium ions have a strong affinity towards these groups containing non-bridging oxygens, which is negative-charged, because they are readily available for charge compensation. Then, the gadolinium ions deform the  $\text{Te-O-Te}$  linkages and change the distribution of ordered microregions of the  $\text{TeO}_2$  crystalline phase.

The EPR spectra of  $x\text{Gd}_2\text{O}_3 \cdot (100 - x)[6\text{TeO}_2 \cdot 4\text{B}_2\text{O}_3]$  glass ceramics sample treated at  $475^\circ\text{C}$  were illustrated in the Fig. 6. These results show the increase of the resonance line ( $g \approx 4.8$ ) attributed to the type of  $\text{Gd}^{3+}$  ions which can be presented as network former in the glass ceramics.

Moreover, we observed a weak resonance line attributed the  $g \approx 2$  due to formation of  $\text{Gd}^{3+}$  clusters for all glass ceramics samples. The weak resonance line  $g \approx 6$  was considered to be a charac-

teristic feature of intermediate crystal field sites of axial symmetry and have attributed the broadened general appearance of the U-spectrum to isolated rare earth ions in wide varieties of sites. The  $\text{Gd}^{3+}$  ions in these glass ceramics can be considered as isolated in the sense of the absence of clustering. The weakening intensity of the clusters EPR line could be due to the  $\text{Gd}^{3+}$  migrations inside the glass network. It should lead to the appearance of more  $\text{Gd}^{3+}$  content in network former positions. It can be pointed that the  $\text{Gd}^{3+}$  ions are generally suspected to improve their environment.

In order to understand these results, Figs. 7 and 8 show comparatively the IR and EPR features of the treated samples at  $400$  and  $475^\circ\text{C}$ , respectively. By increasing the treatment temperature up to  $475^\circ\text{C}$ , the evolution of the structure can be explained considering the accommodation of the network with the excess of oxygen and the higher capacity of migration of the gadolinium ions inside the glass ceramics network (Fig. 7). Here the trends of the three main absorption bands located at  $600\text{--}800$ ,  $900\text{--}1100 \text{ cm}^{-1}$  and  $1200\text{--}1500 \text{ cm}^{-1}$  were considered.

With the increase of treatment temperature up to  $475^\circ\text{C}$ , an increasing trend was observed in strength of the band located at about  $780 \text{ cm}^{-1}$ , which belongs to the stretching vibration of the  $\text{Te-O}$  bonds in  $[\text{TeO}_3]$  structural units. This may be attributed to the electrostatic field of the strongly polarizing  $\text{Gd}^{3+}$  ions. The increase of the  $\text{Gd}^{3+}$  ions content leads to the stronger deformation of the  $\text{Te-O-Te}$  linkages, and consequently causes the formation of the  $\text{TeO}_2$  crystalline phase. The broader band near  $1300 \text{ cm}^{-1}$  corresponds to the vibrations of the boron–oxygen rings composed by  $[\text{BO}_3]$  and  $[\text{BO}_4]$  structural units [30]. Therefore the presumption that boron–oxygen rings were formed in the glass ceramics by the connection of oxygen ions between  $[\text{BO}_3]$  triangles and  $[\text{BO}_4]$  tetrahedrons can be made.

For sample with  $x = 30$  mol%  $\text{Gd}_2\text{O}_3$  was observed a decreasing trend of the bands situated in the  $600\text{--}800 \text{ cm}^{-1}$  region towards lower wavenumber. It is highly possible that a  $[\text{TeO}_3] \rightarrow [\text{TeO}_4]$  conversion process takes place. These  $[\text{TeO}_3] \rightarrow [\text{TeO}_4]$  and  $[\text{BO}_3] \rightarrow [\text{BO}_4]$  conversion processes are responsible of the gradual disappearance of the  $\text{TeO}_2$  and  $\text{B}_2\text{O}_3$  crystalline phases.

The characteristic features of the bands centered in the region between  $1200$  and  $1500 \text{ cm}^{-1}$  were changed drastically by increasing of the  $\text{Gd}_2\text{O}_3$  content. The modifications observed in our study are expected to be mainly due to the  $\text{Gd}^{3+}$  ions. It seems that upon the addition of the rare earth ions, some free orthoborate and boroxol units (the band located at about  $1250 \text{ cm}^{-1}$  becomes sharper and pronounced) are also generated. These simple units containing a large number of non-bridging oxygen and boroxol rings are expected to be created if  $\text{Gd}_2\text{O}_3$  behaves as a glass modifier. It is obvious that the oxygen, which becomes non-bridging and acquires a negative charge, will move closer to the connected gadolinium, consequently reducing the positive charge on the gadolinium.

For the bands located in the  $900\text{--}1100 \text{ cm}^{-1}$  region (assigned to the stretching vibration of  $[\text{BO}_4]$  units) found another increasing trend in the strength with the increase of the  $\text{Gd}_2\text{O}_3$  content. This might be due to the formation of the  $\text{Gd-O-B}$  bridging bonds. The accommodation of the network with the excess of oxygen and the higher capacity of migration of the gadolinium ions inside the host network can be associated with the  $\text{Gd}_2\text{O}_3$  behavior as a glass-former by means of the intercalation of  $[\text{GdO}_4]$  entities in the borate–tellurate chains network.

The EPR spectra of the samples treated at  $475^\circ\text{C}$  (Fig. 8) show the presence of the resonance lines attributed to the type of  $\text{Gd}^{3+}$  ions which can be presented as network former in the glass ceramics ( $g \approx 4.8$ ,  $4.3$  and  $3.3$ ). This type of spectrum shows the disordered polycrystalline materials. The behavior seems to be the change for the sample treated at  $400^\circ\text{C}$  (Fig. 8). According to these results, it can be concluded that most of the gadolinium incorporated into the glass ceramics is not located inside clusters and

the  $\text{Gd}^{3+}$  content is distributed into two sites attributed to network modifier (400 °C) and network former (475 °C).

By increasing of the treatment temperature of the studied glass ceramics, the EPR spectra reveal an increase of the content of  $\text{Gd}^{3+}$  ions in network former positions. Therefore,  $\text{Gd}^{3+}$  ions will coordinate more with non-bridging oxygens leading the decreased of the number of individual  $\text{Gd}^{3+}$  ions. It can be pointed that the  $\text{Gd}^{3+}$  ions are generally suspected to improve their environment.

The FTIR and EPR data revealed that the increase of the  $\text{Gd}_2\text{O}_3$  content and of the treatment temperature influences the rearrangement of borate–tellurate framework. The structure of the glass ceramics was changed from the continuous borate–tellurate network to the continuous gadolinium–borate–tellurate network with interconnected through Gd–O–B and Gd–O–Te bridges.

The changes produced by devitrification suggest that the competition between cations of tellurium and boron with non-bridging oxygens to compensate the positive charge of the gadolinium ions explains the drastic modifications of the characteristic features corresponding to the  $[\text{TeO}_3]$  and  $[\text{BO}_3]$  structural units in bandwidth, position and intensity and the appearance the  $\text{B}_2\text{O}_3$  and  $\text{TeO}_2$  crystalline phases, in agreement with X-ray data.

In brief, the gadolinium ions have a strong affinity towards the  $[\text{BO}_3]$  structural units containing non-bridging oxygens, which are negative-charged, because they are readily available for charge compensation. In Fig. 1, the crystallization of the  $\text{B}_2\text{O}_3$  crystalline phase increases with increasing of the gadolinium concentration because the excess of the oxygen yields the formation of free  $\text{BO}_3^{3-}$  orthoborate units capable for charge compensation of the gadolinium ions. In Fig. 4, the behavior seems to be the opposite because the gadolinium ions have also a pronounced affinity towards the  $[\text{TeO}_3]$  structural units yielding to the deformation of the Te–O–Te linkages, the change of the distribution of ordered microregions of the  $\text{TeO}_2$  crystalline phase and the intercalation of  $[\text{GdO}_4]$  entities in the  $[\text{TeO}_4]$  chain network.

The changes produced by devitrification suggest the competition between cations of tellurium and boron with non-bridging oxygens to compensate the positive charge of the gadolinium ions. Thus, gadolinium ions play a dual role of network former (475 °C) and network modifier (400 °C) in the studied samples.

## 5. Conclusions

The structure of  $x\text{Gd}_2\text{O}_3 \cdot (100 - x)[6\text{TeO}_2 \cdot 4\text{B}_2\text{O}_3]$  glass ceramics prepared by melt-quenching method (for  $x = 0\text{--}30$  mol%  $\text{Gd}_2\text{O}_3$ ) was studied by FTIR, EPR spectroscopy and X-ray diffraction.

When a higher content of  $\text{Gd}_2\text{O}_3$  is introduced in the glass ceramics treated at 400 °C, the  $[\text{TeO}_4]$  structural units are transformed to  $[\text{TeO}_3]$  structural units, the content of  $[\text{BO}_4]$  tetrahedral

units are replaced by  $[\text{BO}_3]$  trigonal structural units and a large number of non-bridging oxygen ions from modifying oxide exist in the glass host. These dramatic structural changes lead the apparition of the  $\text{B}_2\text{O}_3$  and  $\text{TeO}_2$  crystalline phases. The increase of the treatment temperature up to 475 °C leads the gradual disappearance of the  $\text{B}_2\text{O}_3$  and  $\text{TeO}_2$  crystalline phases.

The EPR spectra of the studied glass ceramics reveal the presence of line at  $g \approx 4.8$  characterized for  $\text{Gd}^{3+}$  ions in sites of strong crystal fields having a low coordination number. This type of  $\text{Gd}^{3+}$  ions can be presented as network former in the glass ceramics.

These results can explain the particular influence of the gadolinium ions on the homogeneity, stability and accommodation of the glass ceramics network with the excess of oxygen.

## References

- [1] A.G. Evans, J. Am. Ceram. Soc. 65 (1982) 497.
- [2] F.F. Lange, M. Metcalf, J. Am. Ceram. Soc. 66 (1983) 398.
- [3] D.W. Hall, M.A. Newhouse, N.F. Borelli, W.H. Dumbaugh, D.L. Weidman, Appl. Phys. Lett. 54 (1989) 1293.
- [4] K. Gerth, C. Russel, J. Non-Cryst. Solids 221 (1997) 10.
- [5] J. Lorošch, M. Couzi, J. Pelovz, R. Vacher, A. Lavascur, J. Non-Cryst. Solids 69 (1984) 1.
- [6] A.C. Wright, N.M. Vedischeheva, B.A. Shakmatahin, J. Non-Cryst. Solids 192&193 (1995) 92.
- [7] S. Rada, M. Culea, M. Neumann, E. Culea, Chem. Phys. Lett. 460 (2008) 196.
- [8] H.G. Kim, T. Komatsu, J. Mater. Sci. Lett. 17 (1988) 1198.
- [9] M. Sitarz, M. Szumera, J. Therm. Anal. Calorim. 91 (1) (2008) 255.
- [10] S. Rada, E. Culea, M. Culea, J. Mater. Sci. 43 (19) (2008) 6480.
- [11] M.D. Pankova, Y. Dimitriev, M. Arnaudov, V. Dimitrov, Phys. Chem. Glasses 30 (1989) 260.
- [12] A. Jha, S. Shen, M. Naftaly, Phys. Rev. B 62 (2000) 6215.
- [13] S. Rada, M. Culea, E. Culea, J. Phys. Chem. A 112 (44) (2008) 11251.
- [14] I. Kashif, A.A. Soliman, H. Farouk, M. El-Shorpagy, A.M. Sanad, Physica B 493 (2008) 3903.
- [15] S. Rada, M. Culea, E. Culea, J. Non-Cryst. Solids 354 (52–54) (2008) 5491.
- [16] K. Gatterer, G. Pucker, H.P. Fritzer, Phys. Chem. Glasses 38 (1997) 293.
- [17] E.I. Kamitsos, G.D. Chssikos, M.A. Karakassides, J. Phys. Chem. 91 (1987) 1067.
- [18] S. Rada, M. Culea, M. Rada, M. Culea, J. Mater. Sci. 43 (18) (2008) 6122.
- [19] S. Rada, E. Culea, V. Rus, M. Pica, M. Culea, J. Mater. Sci. 43 (10) (2008) 3713.
- [20] I.E. Iton, C.M. Brodbeck, S.L. Suib, G.D. Stucky, J. Chem. Phys. 79 (1983) 1185.
- [21] C. Legein, J.Y. Buzare, G. Silly, C. Jacoboni, J. Phys.: Condens. Matter 8 (1996) 4339.
- [22] I. Ardelean, L. Griguta, J. Non-Cryst. Solids 353 (2007) 2363.
- [23] E. Culea, I. Milea, J. Non-Cryst. Solids 189 (1995) 246.
- [24] E. Culea, L. Pop, S. Simon, Mater. Sci. Eng. B 112 (2004) 59.
- [25] C.M. Brodbeck, I.E. Iton, J. Chem. Phys. 83 (1985) 4285.
- [26] J. Kliava, I. Edelman, A. Potseluyko, E. Petrakovskaja, R. Berger, I. Bruckental, Y. Yeshurun, A. Malakhovskii, T. Zarubina, J. Magn. Magn. Mater. 272–276 (2004) E1647.
- [27] H.J.A. Koopmans, M.M. Perie, B. Niuzenhuijse, P.J. Gallings, Phys. Status Solidi B 120 (1993) 745.
- [28] D. Furniss, E.A. Harris, D.B. Hollis, J. Phys. C: Solid State Phys. 20 (1987) L147.
- [29] E. Malchukova, B. Boizot, D. Ghaleb, G. Petite, J. Non-Cryst. Solids 352 (2006) 297.
- [30] E.N. Boulos, N.J. Kreidl, J. Am. Ceram. Soc. 54 (1971) 368.